Projected Changes in Rainfall Over Uganda Based on CMIP6 Models

Hamida Ngoma
Brian Ayugi
Charles Onyutha
Hassen Babaousmail
Kenny Lim Sian
Vedaste Iyakaremye
Richard Mumo
Victor Ongoma (victor.ongoma@gmail.com)
Mohammed VI Polytechnic University: Universite Mohammed VI Polytechnique https://orcid.org/0000-0002-5110-2870

Research Article

Keywords: Rainfall, CMIP6, Climate change, Sustainable developement, Uganda

Posted Date: April 1st, 2022

DOI: https://doi.org/10.21203/rs.3.rs-894721/v1

Abstract

Information about likely future patterns of climate variables is important in climate change mitigation and adaptation efforts. This study investigates future (2021–2100) changes in rainfall based on CMIP6 datasets over Uganda. The projection period was divided into two sub-periods: 2021–2060 (near future) and 2061–2100 (far future), relative to the baseline period (1985–2014). Two emission scenarios: SSP2-4.5 and SSP5-8.5, were considered. The results reveal a larger decrease (increase) in rainfall during March – April (November – December) under both SSPs. Moreover, an enhanced decline (increase) is projected under SSP2-4.5 (SSP5-8.5). The spatial distribution of future changes in seasonal rainfall reveals a decrease in MAM rainfall in the near future over most parts of the country under both emission scenarios. However, a recovery is exhibited towards the end of the century with more increase in the south-western parts of the country, and a higher magnitude under SSP5-8.5. In contrast, SON rainfall reveals wetter conditions during both timelines and emission scenarios. Maximum (minimum) wet conditions are expected in the north-western parts of the country (around the Lake Victoria basin). The linear trend analysis shows a non-significant (Z = -0.714) decreasing trend for MAM rainfall during the historical period. This pattern is reflected in the near future with z-scores of -0.757 and − 1.281 under SSP2-4.5 and SSP5-8.5, respectively. However, a significant increase for MAM and annual rainfall (z-scores of 2.785 and 3.46, respectively) is projected towards the end of the century under SSP5-8.5. These findings provide guidance to policy makers in devising appropriate adaptation measures to cope with expected changes in the local climate. Given the increase in intensity and frequency of extreme rainfall over the study region, future work should focus on examining projected changes in rainfall extremes under different global warming scenarios with consideration of model performance and independence.

1. Introduction

Climate variability and change in Uganda and the entire Great Horn of Africa are areas of concern due to their impacts on the economy that largely depends on rainfed agriculture (Limantol et al. 2016; Onyutha 2018; 2019). Uganda has witnessed extreme weather events manifesting as droughts and floods resulting from below and above-normal or heavy rainfall, respectively, in the past years (Mulinde et al. 2016; Ojara et al. 2020). The events had devastating impacts on community livelihoods leading to the displacement of people, loss of lives, and destruction of property. The recent incident is the flooding in late 2021 that significantly affected over 40,000 people (Reliefweb 2021). This among other weather and climate hazards slowdown socioeconomic development, threatening the realization of most sustainable development goals.

Uganda and the East African region at large experience two distinct rainfall seasons, the March to May (MAM ‘long rains’) and the September to November (SON ‘short rains’) seasons (Ayugi et al. 2016; Ongoma and Chen 2017; Ayugi et al. 2018; Ngoma et al. 2021a). The two coincide with the passage of the Intertropical Convergence Zone (ITCZ; Nicholson 2018). The former season is characterized by more rainfall than the latter, because the ITCZ moves faster over the region during SON than MAM. In addition, SON rainfall has been reported to exhibit higher inter-annual and inter-decadal variability compared to

MAM (Hastenrath et al. 1993; Saji et al. 1999), owing to its linkage to global teleconnections such as the El-Niño Southern Oscillation (ENSO) and Indian Ocean Dipole (IOD) (Nicholson and Kim 1997; Ogwang et al. 2015; Ngarukiyimana et al. 2017; Endris et al. 2019; Ngoma et al. 2021b).

Past studies have reported a decreasing (increasing) trend in MAM (SON) rainfall (Camberlin et al. 2003; Onyutha 2016; Nsubuga et al. 2014, 2017; Ongoma and Chen 2017; Ngoma et al. 2021b). The drying trend in the MAM season has been attributed to anthropogenic processes and internal climate variability such as ENSO and Interdecadal Pacific Oscillation (Lyon 2014; Tierney et al. 2015). On the other hand, the wetting pattern for the short rains is linked to the large-scale weakening of the Walker circulation (Williams and Funk 2011; Liebmann et al. 2014; Tierney et al. 2015). Contrary to the current climatic condition which is characterized by several drought events across East Africa, a number of studies using model simulations show that the current is wet and will get wetter in future, a situation that has been termed as the 'East African climate paradox' (Rowell et al. 2015; Ongoma et al. 2018). This paradox has confused policy makers on what ought to be considered in preparing for future changes in rainfall patterns.

General circulation models (GCMs) are used to project climate patterns as they give an insight into the Earth's likely response to warming induced by anthropogenic greenhouse gas (GHG) emissions (Stouffer et al. 2016). One set of GCMs is the Coupled Model Intercomparison Project (CMIP) outputs (Gates et al. 1999), used widely in climatological and hydrological studies. CMIP outputs have evolved over the years, with the latest being phase six (CMIP6) (Eyring et al. 2016). Future changes in the CMIP6 data gives a range of future GHG and land use change scenario estimated from integrated assessment models and based on various assumptions regarding economic growth, climate mitigation efforts, and global governance (Riahi et al. 2017). Recent studies that have utilized CMIP6 reported that the models exhibit improvements compared to CMIP5 (Akinsanola et al. 2020, 2021; Luo et al. 2020; Almazroui et al. 2020; Zhu et al. 2020; Ayugi et al. 2021).

Over Africa, Almazroui et al. (2020) employed 27 GCMs of CMIP6 under three emission scenarios and demarcated the region under 8 zones as recommended by the Intergovernmental Panel on Climate Change (IPCC). The study projected an increase in rainfall over East Africa, where Uganda is located. However, the study considered a broader domain that may not clearly picture the local climate changes. Past studies conducted over East Africa, including Tierney et al. (2015) and Ongoma et al. (2018), based on CMIP5, projected an increase in rainfall which will be higher in the short rains than the long rains. Tierney et al. (2015) further reported a likely decrease in June to August (JJA) rainfall. A recent study based on CMIP6 over the East African region focused mainly on the evaluation of CMIP6 models in simulating mean or extremes rainfall (Akinsanola et al. 2021; Makula and Zhou 2021; Ngoma et al. 2021c) or projections of precipitation extremes over broader East Africa (Ayugi et al. 2021b). However, IPCC (2013) and numerous studies have reported better performance of GCMs in simulating mean rainfall than extreme events (Sillman et al. 2013; Zhang et al. 2016).

Studies conducted over Uganda (e.g., Nsubuga et al. 2014; GOU 2015; Onyutha et al. 2016; Nsubuga and Rautenbach 2017; Egeru et al. 2019; Nimusiima et al. 2019; Ngoma et al. 2021a) projected an increase in rainfall during SON and December to February (DJF). Ngoma et al. (2021a) employed five regional climate models (RCMs) derived from CORDEX-Africa to project future rainfall patterns for the period 2020–2050 under the worst-case scenario (representative concentration pathway, RCP8.5). The results revealed the likelihood of wet conditions in April-May and October, while drier conditions were projected in March. Furthermore, the study projected a decrease (increase) in MAM (SON). Other studies focused on smaller sub-regions of Uganda to examine the projected changes in rainfall or temperature based on CMIP5 outputs (Nimusiima et al. 2014; Egeru et al. 2019). Many of the aforementioned studies focused on extreme rainfall and considered small sub-regions of the country. Occasionally, few studies have considered Uganda as a whole. Nevertheless, the region has quite a few distinct features from the broader East Africa region, such as the mesoscale effect and the short rain season of SON, where the rains start early than most regions of East Africa where the rainfall season is dominant in OND (Nsubuga and Rautenbach 2017; Ngoma et al. 2021a). Importantly, only one study at present has utilized the CMIP6 outputs over Uganda but focused only on few water management zones of Uganda (Onyutha et al. 2021). A number of previous studies on climate change impacts on precipitation in Uganda were based on old generation(s) of the GCMs, especially those from phases 3 (CMIP3) and CMIP5.

With advent of CMIP6 models, that includes more comprehensive global climate models with generally more sophisticated physics and higher resolution, which is anticipated to yield a better capability of representing real climate systems. Moreover, the shared socioeconomic pathways (SSPs; O`Neill et al. 2017) provides additional descriptions of socioeconomic development, unlike the previous versions of representative concentration pathways (RCPs; Van Vuuren et al. 2011) that only captured the projections of the components of radiative forcing for use for assessment of changes in climate system. Subsequently, these SSPs were considered in the preparation of latest Sixth Assessment Report (AR6; IPCC 2021) where they are being utilized to examine how the societal actions will impact on the emissions of GHGs and also how climate goals under Paris Agreement will be attained.

Thus, there is a need for accurate and reliable information on future rainfall patterns for informed decision-making and planning in climate sensitive sectors such as agriculture, energy and health. Other than helping to formulate effective adaptation measures to the climate climate, the information is key in devising relevant climate change mitigation strategies. The improved performance in CMIP6 as compared to CMIP5 presents promising reliability of the models in projecting the East African regions' climate. The key scientific questions to address are: (1) What are the future characteristics of rainfall over Uganda as projected by the best-performing CMIP6 GCMs? (2) How will future rainfall patterns over Uganda vary under the worst-case scenarios? Section 2 gives a brief description of the study domain, the data and methods employed in the study. Section 3 presents the findings, while Section 4 enumerate the discussions of the study. Lastly, the conclusion and possible recommendations are outlined in Section 5.

2. Study Area, Data And Methods

2.1 Study Area

Uganda is situated in the east of Africa (Fig. 1). Its elevation varies from complex topography ranging from low-lying areas in the west along the Rift Valley, flat land in the north and highland regions in the southwest and eastern parts of the country. The highest altitude is on the southwest (Mts. Rwenzori and Mufumbira) and east (Mt. Elgon and Moroto). The southern part of the country comprises tropical landscapes. However, moving northward towards South Sudan, the landscape becomes increasingly flat and dry, with widespread savannah and thorn bush landscapes. Other geographical features of Uganda include Africa's largest freshwater lake, Lake Victoria, as well as Lakes Kyoga, Albert, George and Edward, and Africa's longest river, River Nile. All these features influence the local weather and climate over the region. The rainfall seasonality is mainly influenced by the ITCZ, which oscillates northward and southward, crossing the Equator twice in a year.

Other systems influencing rainfall over the region include the subtropical anticyclones, ENSO, quasi-biennial oscillation (QBO), tropical monsoons, IOD and moist westerlies from the Congo Basin (Basalirwa 1995). The country's annual rainfall ranges between 750 and 2500 mm per year, with the highest amounts received in the Lake Victoria basin (NEMA 2008). The start of the rainy seasons can shift by 15 to 30 days from an average year, making it difficult for farmers to determine the best time for planting. Uganda's economy largely depends on rainfed agriculture and 96% of all farmers in Uganda are considered smallholders, contributing 75% of the country's total agricultural production (WFP 2016). The leading crops produced in Uganda are beans, cassava, sweet potatoes, coffee, groundnuts, maize, millet, sorghum, sesame and *matoke* - plantain banana (NBER 2010), grow in distinct climatic zones.

2.2 Data

The multi-model ensemble (MME) of six CMIP6 models was utilized in the present study. The models were chosen based on their ability to simulate rainfall over Uganda (Ngoma et al. 2021c). The use of MME reduces the uncertainties and made climate projection more reliable (Knutti et al. 2010). The underlying assumptions of the multi-model ensemble mean practice is that all models are reasonably independent, equally plausible, and distributed around the reality (Sanderson et al. 2015; Knutti et al. 2017). It also assumes that the range of model projections is representative of what we believe is the uncertainty. Many studies have thus employed MME as a way of minimizing the uncertainity in the projections of rainfall over various regions (Tebaldi and Knutti 2007; Ayugi et al 2021b; Lim Kan Sian et al. 2021). Table 1 summarizes the models employed, their developing institutions, horizontal resolution and main reference(s). The model data can be accessed from the Earth System Federation portal at https://esgf-node.llnl.gov/search/cmip6. The first realization members (r1i1p1f1) of the models for both SSP scenarios were chosen for projections. The models were then re-gridded to a common grid of 1°×1° resolution using a remapping procedure of distance weighted average. The aforesaid technique interpolation follows better classification of diverse geography through data triangulation of nearest points and sub-regionalization of grid points by the nearest cell center input grids thereby suitable for comparative analysis from uniform grids (Varmeulen et al. 2017).

Table 1
CMIP6 models employed in the study, and their modeling centers, horizontal resolutions and main references.

No	Models	Institution	Resolution	Reference
1	CanESM5	Canadian Centre for Climate Modelling and Analysis, Environment and Climate Change Canada, Victoria, Canada	2.81º×2.81º	(Swart et al., 2019)
2	CESM2-WACCM	National Center for Atmospheric Research, USA	1.25º × 0.94º	(Danabasoglu et al., 2019)
3	CNRM-CM6-1	Centre National de Recherches Météorologiques (CNRM); Centre Européen de Recherches et de Formation Avancée en Calcul Scientifique, France	1.41 º × º 1.41 º	(Voldoire et al., 2019)
4	GFDL-ESM4	Geophysical Fluid Dynamics Laboratory (GFDL), USA	1.25º×1.00º	(Krasting et al., 2018)
5	MRI-ESM2-0	Meteorological Research Institute (MRI), Japan	1.13º×1.13º	(Yukimoto et al., 2019)
6	NorESM2-LM	Norwegian Climate Centre/Norway	1.875º × 2.5 º	(Seland et al., 2020)

Rainfall projections were analyzed based on two emission scenarios: SSP2-4.5 and 5-8.5, representing medium forcing and policy, and worst-case; no policy scenario, respectively. Table 2 gives more details about the SSPs. The scenarios are based on new future pathways of societal development (SSPs; O'Neill et al. 2017) and related to RCPs (van Vuuren et al. 2011).

Table 2

Emission scenarios employed in the study.

SSP	Forcing
SSP2-4.5	Medium part of the future forcing pathways range; updates the RCP4.5 pathway with 4.5 W/m^2 forcing
SSP5-8.5	High end of the future pathways range in the IAM literature; updates the RCP8.5 pathway with 8.5W/m^2 forcing

Monthly rainfall data from the Climate Hazards Group Infra-Red Rainfall with Station (CHIRPS) (Funk et al. 2015) was used to validate the models' simulation of rainfall climatology over the region. The data covers a period of 1981-present and has been evaluated and appraised over the region (Dinku et al. 2018; Ayugi et al. 2019; Ngoma et al. 2021a).

2.3 Methods

Rainfall projection for both SSPs was considered during two time slices: 2021–2060 (near future) and 2061–2100 (far future) relative to a baseline period in order to compare changes in the near future and

towards the end of the century. The changes are evaluated relative to the latest baseline period of 30 years (1985–2014). The models' historical simulation was first compared with CHIRPS data to validate their performance in simulating the monthly annual cycle over the region during the baseline period. Future changes in monthly rainfall were then assessed for both time slices under the two emission scenarios. The projected changes were quantified in percentage of the baseline mean rainfall. Furthermore, a projected spatial rainfall anomalies analysis was performed for the two rainfall seasons. Inter-annual and intra-seasonal variation of future changes in rainfall over the whole study period was computed and presented on a portrait diagram.

The modified Mann-Kendall (m-MK) test (Hamed and Rao 1998) was used to detect the significance of projected linear rainfall trends. The significance for m-MK is calculated at 95% confidence level. The m-MK test is preferred over the original MK test (Mann 1945; Kendall 1975) because it incorporates missing values in a time series and it also employs relative magnitudes rather than numerical values that allows 'trace' or 'below' detection data (Hirsch et al. 1993). The approach has been employed by various hydrological and climatological studies (e.g., Tadeyo et al. 2020; Tan et al. 2020; Ongoma et al. 2021; Ngoma et al. 2021c; Ayugi et al. 2021). The Theil-Sen's slope estimator (Theil 1950; Sen 1968) was used to measure and compare the magnitude of projected rainfall against the baseline period over the study domain. The method is considered effective since it is not influenced by any extreme distribution and does not entail any normal distribution of the residuals. Furthermore, the sequential Mann-Kendall (SQMK) test (Sneyers 1990) was carried out to determine abrupt changes in seasonal and annual projected rainfall. Several climatological studies have successfully employed the technique (e.g., Mumo et al. 2019; Ngoma et al. 2021a, b; Ayugi and Tan 2019; Lim Kam Sian et al. 2021).

Probability density functions (PDFs) for seasonal and annual mean monthly rainfall were computed for the baseline and projections periods under both emission scenarios. PDFs are used to show how variability, skewness and distribution of a variable may change under a shifting climate (Stott et al. 2016).

3. Results And Discussions

3.1 Monthly annual cycle

Figure 2 shows the monthly annual cycle of future rainfall under SSP2-4.5 and SSP5-8.5 scenarios, alongside the models' ensemble and observed historical period. It is apparent that highest amount of rainfall is received in November while the least amount is in July in CMIP6 models. However, CHIRPS records the maximum amount of rainfall in April (153.14 mm) while the minimum amount is witnessed in January (40 mm). Projections under SSP5-8.5 scenarios for far future point to higher rainfall relative to the baseline period than under the SSP2-4.5 scenario. Remarkably, the models reproduce the expected bimodal rainfall pattern following the north-south oscillation of the tropical belt across the region (Nicholson 2018). Meanwhile, the models slightly overestimate January to April rainfall and highly

underestimate (overestimate) June to August (October to December) rainfall during the historical period. January to May, and September reveal minimal model biases.

Projections under the SSP2-4.5 emission scenario reveal a decrease (increase) in rainfall between January and April (May to December) in the near future. Notably, the increase rate is higher than for the projected decrease. In addition, SSP5-8.5 for the same period projects a slight increase in wet conditions for January at 3.35 mm and February at 3.59 mm whilst a decrease in March to April rains is observed at -0.76 mm relative to the baseline period. Nevertheless, a high increase for the rest of the months is noted in the model projection under SSP2-4.5 and SSP5.85 scenarios. Towards the end of the century, SSP2-4.5 projects relatively more increase in rainfall than in the near future. Wetter conditions are depicted in all months except for March and April, revealing a reduction in rainfall during this period. On the other hand, SSP5-8.5 projects an increase in monthly rainfall in the far future. Overall, the models project an increase in rainfall over Uganda between 2021–2100, except for March and April. A more pronounced increase will be experienced under the high emission scenario towards the end of the century compared to that of the near future.

<Fig. 2>

3.2 Spatio-temporal variability of projected change in rainfall

To assess the spatio-temporal variability of future rainfall, seasonal change in rainfall for MAM and SON is analyzed by establishing the difference in future rainfall patterns relative to the baseline period of 1985–2014. Figures 3 and 4 show the projected changes in the spatial distribution of rainfall for MAM and SON, respectively, for the near future and far future under SSP2-2.5 and SSP5-8.5 scenarios. Under SSP2-4.5, MAM rainfall is projected to decrease over the entire country in the range of 0–4 mm (Fig. 3). The highest reduction in rainfall will be experienced in the eastern parts of the country around Mts. Elgon and Moroto, while the least will be in the south-western parts of the Kabale Highlands. Most parts of the country are expected to experience less MAM rains (< 4–8 mm) relative to the reference period. Although the SSP5-8.5 scenario equally projects a decrease in rainfall in the near future over most parts of the country, the magnitude of the reduction is less than that under SSP2-4.5. An increase in the western part of the study domain is also expected. Similarly, the south-western region exhibits more increase compared to other parts of Uganda. Towards the end of the century, SSP2-4.5 projects an increase in rainfall of up to 8 mm in the southern and western parts of the country, and a decrease in the eastern part, except around the Lake Victoria region. In addition, it is evident that under SSP5-8.5 scenario, future projections show an increase in MAM rainfall over the entire country in the far future. Nevertheless, the highest decrease is demonstrated in the south-western parts. The increase is expected to be between 8 and 24 mm and increases westwards.

<Fig. 3**>**

Projected changes for SON rainfall depict wetter conditions over the entire country in both timelines under both scenarios (Fig. 4). For the near future, the increase in rainfall increases westwards. The intensity under SSP5-8.5 is higher than that under SSP2-4.5. The SSP2-4.5 (SSP5-8.5) exhibits an increase of 0–30 (5–40) mm. Less wet conditions are noted in the Lake Victoria region, which has been known to receive more rainfall than other parts of the country. Towards the end of the century, both scenarios project wetter conditions over the region as compared to the near future. More wetness will be experienced in the northern parts. These regions are arid and semi-arid lands (ASALs), receiving relatively low rainfall than other parts of the country. Furthermore, similar patterns to the near future are exhibited in the southern parts, where the smallest increase is depicted. These results agree with the findings of Nsubuga and Rautenbach (2017) that projected wet conditions over the west and north-western parts of the country and a drop in rainfall over the Lake Victoria region.

<Fig. 4**>**

Further analysis for future rainfall changes in the next 80 years was conducted on a temporal scale to investigate rainfall inter-annual and intra-seasonal variability. Figure 5 shows the portrait diagram for future changes in rainfall relative to the reference historical period under the two scenarios. The results show high inter-annual and intra-seasonal variability under both scenarios. Under the SSP2-4.5 scenario, January – April show drier conditions, especially in the near future. More decrease in rainfall is projected during March and April. April shows the highest decrease with wet spells oscillation periods of 5–7 years. This could be linked to ENSO, which exhibits a similar cycle (Nicholson 2015). September to December show the wettest conditions, and the intensity and frequency increase towards the end of the century. Furthermore, November depicts a higher increase of > 100% for many years, except 2030, 2031 and 2061, which reveal drier conditions relative to the reference period. October 2029 also projects a high increase in rainfall (134%). June – August project minimal changes in rainfall throughout the study period. Under SSP5-8.5, wetter conditions are expected than SSP2-4.5. November and December show wetter conditions with few dry conditions throughout the century. Drier conditions are evident during March and April, but they will get wet in the last decade. January is also projected to become wetter in the far future, which might extend the SON season. Overall, more rainfall is projected towards the end of the century under both emission scenarios.

<Fig. 5**>**

3.3 Projected trend of rainfall

Future spatial rainfall trends were analyzed and compared against the historical baseline for MAM and SON seasons (Figs. 6 and 7). The historical period reveals a decreasing trend of 0 to -4 mm in rainfall during MAM over most parts of the country, except a small region in the southwest which shows an increasing trend of up to 0.2 mm. Under SSP2-4.5, rainfall in the near future is expected to decrease, but the magnitude will be higher in the southern parts of the country. On the contrary, SSP5-8.5 projects more rainfall reduction in the range of 0-1.2 mm and a slight increase in the north-western part. Towards the end of the century, both scenarios project an increasing trend in MAM rainfall over the whole country.

However, the increase is higher under SSP5-8.5 and the magnitude increases westward. On the other hand, SON rainfall exhibits a slight increasing trend during the baseline period over the country. The SSP2-4.5 projects almost similar patterns in the near future as the historical period. In addition, SSP5-8.5 reveals an increasing trend which is higher in the north-eastern parts of the country. For the far future, SSP2-4.5 projects a slight increasing (decreasing) trend over most (southern and north-western) parts of the country. Furthermore, SSP5-8.5 reveals an increasing trend with the highest magnitude in the north-western parts of the country.

<Fig. 6**>**

<Fig. 7**>**

The temporal trends were further assessed for MAM, SON and annual. Figure 8 shows the temporal variation and trends for both scenarios at seasonal and annual scales relative to the reference period. MAM season depicts a decreasing trend in the historical period, which is expected to slightly decrease under both scenarios in the near future. However, in the far future, a small and sharp increase is projected under SSP2-4.5 and SSP5-8.5 scenarios, respectively. On the other hand, SON rainfall has been increasing historically and is projected to follow the same trend in the near future under both emission scenarios. Moreover, contradicting trends are projected by the two scenarios towards the end of the century. SSP2-4.5 shows a slightly decreasing trend, whereas SSP5-8.5 reveals an increasing trend. On an annual scale, the historical baseline period simulates an increasing trend,which is projected to persist in the near future under the two scenarios. However, towards the end of the century, a sharp increasing trend is expected in the annual rainfall over the region.

Results in Fig. 8 show that trend slope can change with respect to both magnitude and sign based on the period selected for analysis. In other words, if the trend was fitted to the entire 2021–2100 future climatic data, one would miss out on the relevant information regarding the sub-trends (Onyutha 2021). The variation in rising and falling sub-trends over the various sub-periods indicates random large-scale fluctuations in the climatic data (Onyutha 2021). This means there is a need to consider both climate variability and change when analyzing climate variables. Furthermore, the characterization of natural variation in terms of the statistical dependence is relevant in determining how well the climate models reproduce the variability in the observed rainfall and other climatic variables (Onyutha et al. 2018).

<Fig. 8**>**

The m-MK test and Theil-Sen's slope estimator were employed to test the significance and magnitude of projected rainfall trends, respectively, at $\alpha = 0.05$. Table 3 summarizes the mean, slope and Z-score of seasonal and annual rainfall for the baseline period, and near and far future under both scenarios. The MAM season depicts decreasing trend for the baseline period and in the near future for both emission scenarios. However, an increasing trend is projected in the far future under the two scenarios. SSP2-4.5

(SSP5-8.5) projects an insignificant (significant) trend of z-score 0.92 (2.785) or $p > 0.05$ ($p < 0.05$). In addition, SON rainfall reveals an insignificantly increasing trend for all periods under both scenarios, including the baseline period. Annual rainfall also shows increasing trends for all cases, which is only significant towards the end of the century under SSP5-8.5 with a z-score of 3.46 ($p < 0.01$). Overall, rainfall is projected to increase during MAM, SON and at annual scale, except for MAM near future. However, MAM and annual rainfall project a significant increase in the rainfall trend. These findings agree with previous studies (Nimusiima et al. 2014, 2019; Ongoma et al. 2018; Egeru et al. 2019) conducted over East Africa or smaller regions of Uganda.

Table 3
Projected linear trend for MAM, SON and annual precipitation between 2021–2100 relative to the baseline period (1985–2014). The asterisks represent data at 95% confidence level.

Period	MAM			SON			ANNUAL		
	mean	slope	Z-score	mean	slope	Z-score	mean	slope	Z-score
Baseline	132.0	-0.015	-0.714	154.09	0.015	0.642	104.61	0.026	1.799
SSP2-4.5 Near	125.39	-0.010	-0.757	171.62	0.016	1.596	111.39	0.028	1.829
SSP5-8.5 Near	130.26	-0.006	-1.281	178.14	0.019	1.480	116.63	0.019	1.433
SSP2-4.5 Far	132.18	0.009	0.920	187.06	0.003	0.338	118.77	0.007	0.431
SSP5-8.5 Far	143.63	**0.032***	2.785	195.16	0.013	0.944	129.95	**0.042***	3.460

Figure 9 shows the results of the sequential Mann-Kendall test statistics for MAM and SON rainfall under SSP2-4.5 and SSP5-8.5 scenarios. Overall, the results depict an upward trend during both seasons for the two scenarios, though with varying amplitudes. Under SSP2-4.5, the MAM season projects a decreasing trend at the start until mid-decade, where there is a reversal up to 2029. The trend then decreases again in the second decade, with an abrupt change projected to occur around 2043, significant at $\alpha = 0.05$, implying a significant ($p < 0.05$) decline in rainfall. The trend after that increases throughout the projection period with abrupt but insignificant changes at five different periods. For SSP5-8.5, an increasing trend is initially projected, after which a prolonged reversal decrease will occur until 2060. Later in the far future, a sharp increasing trend is expected towards the end of the century. No abrupt change is projected throughout the period. The SON season and annual rainfall project increasing trends under both emission scenarios without any abrupt change.

<Fig. 9**>**

3.4 Probability density functions

The distribution of future seasonal and annual rainfall over the study domain was compared with that of the baseline period using PDFs. Figure 10 shows the distribution of MAM, SON and annual rainfall displayed as normalized curves under the two scenarios. Under SSP2-4.5, a negative shift with higher variation in MAM rainfall is projected in the near future, whereas the distribution is expected to persist with a slight increase in variation towards the end of the century relative to the reference period. However, SSP5-8.5 projects similar variations with a smaller negative shift in the near future and a greater positive shift towards the end of the century. For SON, SSP2-4.5 reveals a positive shift with an increase in the maximum for both time periods, implying an increase in mean rainfall amount and variability. In addition, the shift and variability will be higher in the far future. Under SSP5-8.5, both time slices reveal a shift to the right in the far future. The peak in the near future is higher, thus more variability is expected. Furthermore, mean annual rainfall depicts a small (larger) positive shift in the near (far) future. The near future reveals a sharp increase in the peak, pointing to less increase in mean annual rainfall but with high variability. SSP5-8.5, on the other hand, projects a positive shift in mean rainfall, but the peak is reduced more in the far future, which means an increase in magnitude. These results are in conjunction with previous studies conducted over East Africa (Anyah and Qiu 2012; Ongoma et al. 2018).

<Fig. 10**>**

4. Discussion

Information on future changes in rainfall is valuable in developing preparedness measures through early warning systems. This study employed the multi-model ensemble of the best-performing models (Ngoma et al. 2021c) to assess future changes in rainfall in the near future (2021–2061) and towards the end of the century under SSPs 2-4.5 and 5-8.5 scenarios. The results reveal that there will be a decline in the MAM rainfall in the near future, whilst an increase in SON and annual rainfall is projected for all the time periods under both emission scenarios (Fig. 2). Notably, rainfall is projected to increase with the increase in atmospheric radiative forcing. The MAM rainfall also reveals a recovery period with a projected increase towards the end of the century under both scenarios (Fig. 2). The findings disagree with previous studies, including Ongoma et al. (2018), which projected an increase in rainfall during March over East Africa based on CMIP5 but agree with Ngoma et al. (2021a). This points out the need for focusing on homogeneous rainfall zones when analyzing their variability. Patricola and Cook (2011) attributed the projected decrease to the weakening of the Somali Jet Stream and Indian Monsoon, and reduction in evaporation. The projected wet patterns in other months, especially OND, are, on the other hand, linked to the weakening of the Walker circulation over the Indian Ocean (King et al. 2021).

Overall, SON rainfall is projected to increase more compared to the MAM rainfall. The results further show that there will be an increase in rainfall from October to December. This might shift or extend the short rainfall season of SON to December in the near future. Previous studies link the models' October to November rainfall overestimation to the poor representation of global teleconnections such as the Walker circulation over the Indian Ocean in the parameterization schemes (Yang et al. 2015; King et al. 2021), and the prominent modes of inter-annual and inter-decadal rainfall variability (Giannini et al. 2008).

According to Sylla et al. (2012), some of these features and systems are poorly understood due to limited access to observations and research attention. None of the current generations of GCMs were developed in Africa and the relevant processes over the continent have not always been a priority during model development. On the other hand, James et al. (2018) argue that the evaluation of climate models over Africa needs to move from scalar metrics, validation, and performance checks to investigating how models simulate processes on a regional scale. This would help in improving the accuracy of future projections. Nevertheless, despite the observed model uncertainties, future projections provide a picture of the expected climate conditions that are needed for long-term planning. The models can therefore be employed to project changes in rainfall over the study region.

Spatial variability reveals a higher positive change during SON as compared to MAM, with notable changes over north-western parts of the country (Figs. 3 and 4). A reduction in rainfall around the Lake Victoria basin is also revealed. These results align with previous studies conducted either over the East Africa region (Ongoma et al. 2018) or at national and sub-regional levels (Egeru et al. 2019; Nsubuga and Rautenbach 2017). The decrease in March and April rainfall has been attributed to a strong southerly Somali jet over the Horn of Africa that turns westerly over the Arabian Sea, thereby transporting moisture over EA (Hastenrath et al. 2011). Other studies link the MAM rainfall drying pattern to the weakening of the Walker circulation over the Indian Ocean (Williams and Funk 2011). MAM is the main crop growing season for seasonal crops such as maize, beans, potatoes and ground nuts. A decrease in March and April rainfall could have far-reaching effects on the community's livelihoods. This shift in the MAM season might require a change in the timing of crop planting, and raise the need for adopting drought-resistant or fast-growing crops. Overall, an increase in rainfall is likely to boost agricultural productivity, especially in ASALs that are generally characterized by fertile soils and limited rainfall. This would support farming across the whole country, as the main producers are located in the southern part of the country. Crops such as beans, bananas, potatoes, and cassava, which are only grown in wet areas are likely to survive in the northern parts of the region under the projected increase in rainfall. On the other hand, the wetter conditions projected in the south-western parts of the country might increase the occurrence of floods as this region comprises highlands that has been prone to floods in recent years (Nsubuga et al. 2014).

Meanwhile, it should be noted that the findings of the study might not give accurate climate conditions as the models may under/overestimate rainfall for both scenarios. This is mostly attributed to the low resolution of the models and the poor representation of systems influencing inter-annual and intra-seasonal variability of rainfall over the study domain. Notably, both the current models and the predecessor (CMIP3/5) tend to overestimate the short rains while underestimating the long rains over East Africa (Anyah and Qiu 2012; Ongoma et al. 2018; Ngoma et al. 2021c). Nevertheless, the results of this study would contribute to the ever-present debate on expected projected changes in the region's rainfall variation. The projections continue to draw much attention because they give opposite patterns to the observed rainfalls. The results can be utilized by relevant stakeholders, including policymakers and farmers. Policymakers should design appropriate policies that reflect all possible outcomes as various studies are inconclusive on the exact direction of future climate in the wake of global warming and

climate change. Although it is imperative to examine the changes in mean rainfall over the study region, the ever-increasing occurrences of extreme rainfall events in recent years call for a shift in analysis to examine extreme events in Uganda. Thus, future studies are recommended to focus on projected changes in rainfall extremes under different global warming scenarios while considering model performance and independence for accurate projections.

5. Conclusion

Annual climatology from the CMIP6 models shows that the highest amount of rainfall is received in November while the lowest amount is in July. Projections under the SSP2-4.5 emission scenario reveal a decrease (increase) in rainfall between January and April (May to December) in the near future, whereas under SSP5-8.5 scenarios, high rainfall occurrence is expected. The models project an increase in rainfall over Uganda between 2021–2100, except during March and April. However, a more pronounced increase will be experienced under the high emission scenario towards the end of the century.

Spatial changes during MAM show that the highest reduction in rainfall will be experienced in the eastern parts of the country around Mts. Elgon and Moroto while the least will be in the south-western parts of the Kabale Highlands. Towards the end of the century, SSP2-4.5 projects an increase in rainfall of up to 8 mm in the southern and western parts of the country and a decrease in the eastern part, except around Lake Victoria. In comparison, the highest decrease is expected in the south-western parts, while an increase of 8 to 24 mm is expected westwards between 8 to 24 mm under SSP5-8.5 scenario. During the SON season, projected changes depict wetter conditions over the entire country in both timelines under the two scenarios.

Spatial trends depict an increasing pattern in MAM rainfall over the country relative to the baseline period that showed a declining tendency of 0 to -4 mm. SSP5-8.5 scenario reveals an increasing trend with the highest magnitude in the north-western parts of the country. Temporal changes based on Theil-Sen's slope estimator show SSP2-4.5 (SSP5-8.5) projects an insignificant (significant) trend of z-score 0.92 (2.785) or $p > 0.05$ ($p < 0.05$) during MAM. Modified Mann-Kendall test shows no abrupt change is projected throughout the period. SON and annual rainfall project increasing trends under both emission scenarios without any abrupt change.

Lastly, a comparison of future seasonal and annual rainfall over the study domain relative to the baseline period was conducted using PDFs. Under SSP2-4.5, a negative shift with higher variation in the MAM rainfall is projected in the near future, whereas the distribution is expected to persist with a slight increase in variation towards the end of the century relative to the reference period. For SON, SSP2-4.5 reveals a positive shift with an increase in the maximum for both periods, implying an increase in mean rainfall amount and variability. Mean annual rainfall depicts a slight (larger) positive shift in the near (far) future.

Declarations

Acknowledgments

The lead authoris grateful to the Nanjing University of Information Science and Technology (NUIST) for providing a favorable working environment, and structural and technological support for conducting the research.

Funding Statement

The corresponding author was supported by a research grant from Mohammed VI Polytechnic University under the research grant to professors with grant number UM6P.

Author's Contribution

HN, BA, VO: Conceptualization, manuscript writing, results verification. CO and HB: data analyses and manuscript correction. KLS: conceptualization and manuscript correction. VI and RM: results verification and manuscript correction.

Data availability

The CMIP6 data used in this study can be accessed at no cost from the Earth System Federation portal at https://esgf-node.llnl.gov/search/cmip6. Rainfall data from the Climate Hazards Group Infra-Red Rainfall with Station (CHIRPS) is also freely available at https://www.chc.ucsb.edu/data/chirps.

Code availability

The data analysis codes are available from HN,BAand HB, and can be shared on request.

Ethics approval and consent to participate

Not applicable

Consent for publication

Consents for publication from all the co-authors are received.

Conflict of interest

The authors declare no competing interests.

References

1. Akinsanola AA, Kooperman GJ, Pendergrass AG, Hannah WM, Reed KA (2020) Seasonal representation of extreme rainfall indices over the United States in CMIP6 present-day simulations. Environ Res Lett 15, 094003. https://doi.org/10.1088/1748-9326/ab92c1

2. Akinsanola AA, Ongoma V, Kooperman GJ (2021) Evaluation of CMIP6 models in simulating the statistics of extreme precipitation over Eastern Africa. Atmos Res 254, 105509. https://doi.org/10.1016/j.atmosres.2021.105509
3. Almazroui M, Saeed S, Saeed F, Islam MN, Ismail M, Klutse NAB, Siddiqui MH (2020) Projected Change in Temperature and Rainfall Over Africa from CMIP6. Earth Syst Environ 4: 455–475. https://doi.org/10.1007/s41748-020-00161-x
4. Anyah RO, Qiu W (2012) Characteristic 20th and 21st century rainfall and temperature patterns and changes over the Greater Horn of Africa. Int J Climatol32: 347–363. https://doi.org/10.1002/joc.2270
5. Ayugi B, Dike V, Ngoma H, Babaousmail H, Mumo R, Ongoma V (2021b). Future changes in precipitation extremes over East Africa based on CMIP6 projections. Water *13*(17), 2358. https://doi.org/10.3390/w13172358
6. Ayugi B, Jiang V, Zhu H, Ngoma H, Babaousmail H, Karim R, Dike V (2021a) Comparison of CMIP6 and CMIP5 models in simulating mean and extreme rainfall over East Africa. Int J Climatol 41:6474–6496. https://doi.org/10.1002/joc.7207
7. Ayugi B, Ngoma H, Babaousmail H, Karim R, Iyakaremye V, Lim Kam Sian KTC, Ongoma V (2021c) Evaluation and projection of mean surface temperature using CMIP6 models over East Africa. J Afri Earth Sci 181, 104226. https://doi.org/10.1016/j.jafrearsci.2021.104226
8. Ayugi B, Tan G, Ullah, W, Boiyo R, Ongoma V (2019) Inter-comparison of remotely sensed precipitation datasets over Kenya during 1998–2016. Atmos Res 225: 96–109. https://doi.org/10.1016/j.atmosres.2019.03.032
9. Ayugi BO, Tan G, Ongoma V, Mafuru KB (2018) Circulations Associated with Variations in Boreal Spring Rainfall over Kenya. Earth Syst Environ2: 421–434. https://doi.org/10.1007/s41748-018-0074-6
10. Ayugi BO, Wang W, Chepkemoi D (2016) Analysis of Spatial and Temporal Patterns of Rainfall Variations over Kenya. Environ Earth Sci 6: 69–83.
11. Basalirwa CPK (1995) Delineation of Uganda into climatological rainfall zones using the method of principal component analysis. Int J Climatol15: 1161–1177. https://doi.org/10.1002/joc.3370151008
12. Camberlin P, Okoola RE (2003) The onset and cessation of the “long rains” in eastern Africa and their interannual variability. Theor Appl Climatol 54: 43–54, https://doi.org/10.1007/s00704-002-0721-5.
13. Danabasoglu G (2019) NCAR CESM2-WACCM model output pre- pared for CMIP6 CMIP historical. Earth System Grid Federation. Version 20200420. https://doi.org/10.22033/ESGF/CMIP6.10071.
14. Dinku T, Funk C, Peterson P, Maidment R, Tadesse T, Gadain H, Ceccato P (2018) Validation of the CHIRPS satellite rainfall estimates over eastern Africa. Q J R MeteorolSoc 144 (Suppl. 1): 292–312. https://doi.org/10.1002/qj.3244
15. Egeru A, Barasa B, Nampijja J, Siya A, Makooma MT, Majaliwa MGJ (2019). Past, present and future climate trends under varied Representative Concentration Pathways for a sub-humid region in

Uganda. Climate 7, 35. https://doi.org/10.3390/cli7030035

16. Endris HS, Lennard C, Hewitson B, Dosio A, Nikulin G, Artan GA (2019) Future changes in rainfall associated with ENSO, IOD and changes in the mean state over Eastern Africa. ClimDyn 52: 2029–2053. https://doi.org/10.1007/s00382-018-4239-7
17. Eyring V, Bony S, Meehl GA, Senior C, Stevens B, Stouffer RJ, Taylor KE (2016) Overview of the Coupled Model Intercomparison Project Phase 6 (CMIP6) experimental design and organisation. Geosci Model Dev 9: 1937–1958. https://doi.org/10.5194/gmdd-8-10539-2016
18. Funk C, Peterson P, Landsfeld M, Pedreros D, Verdin J, Shukla S, Husak G, Rowland J, Harrison L, Hoell A, Michaelsen J (2015) The climate hazards infrared rainfall with stations - A new environmental record for monitoring extremes. Scientific Data 2: 1–21. https://doi.org/10.1038/sdata.2015.66
19. Gates WL, Boyle JS, Covey C, Dease CG, Doutriaux CM, Drach RS, Fiorino M, Glecker PJ, Hnilo JJ, Marlais SM, Phillips TJ, Potter GL, Santer BD, Sperber KR, Taylor KE., Williams DN (1999) An Overview of the Results of the Atmospheric Model Intercomparison Project (AMIP I). Bull AmericMeteorolSoc 80: 29–56. https://doi.org/10.1175/1520-0477(1999)080<0029:AOOTRO>2.0.CO;2.
20. Giannini A, Lyon B, Seager R and Vigaud N (2018) Dynamical and thermodynamic elements of modelled climate change at the East African margin of convection. Geophys Res Lett 45: 992–1000. https://doi.org/10.1002/2017GL075486
21. Government of Uganda (GOU) 2015. Economic Assessment of the Impacts of Climate Change in Uganda. Final Study Report. Ministry of Water and Environment, Climate Change Department Kampala.
22. Hamed KH, Rao RA (1998) A modified Mann–Kendall trend test for autocorrelated data. J Hydrol 204:182–196.https://doi.org/10.1016/S0022-1694(97)00125-X
23. Hastenrath S, Nicklis A, Greischar L (1993) Atmospheric-hydrospheric mechanisms of climate anomalies in the western equatorial Indian Ocean. J Geophys Res 98(C11): 20219–20235. https://doi.org/10.1029/93JC02330
24. Hastenrath S, Polzin D, Mutai C (2011) Circulation mechanisms of Kenya rainfall anomalies. J Climate 24: 404–412. https://doi.org/10.1175/2010JCLI3599.1
25. Hirsch R, Helsel D, Cohn T, Gilroy E (1993) Statistical analysis of hydrologic data. In: Maidment D (Ed) Handbook of hydrology. McGraw-Hill, New York.
26. IPCC (2001) In *Climate Change 2001: Impacts, Adaptation and Vulnerability, Contribution of Working Group II to the Third Assessment Report of the Intergovernmental Panel on Climate Change*. McCarthy JJ, Canziani OF, Leary NA, Dokken DJ, White KS (eds). Cambridge University Press: Cambridge, UK and New York, NY, 1032.
27. IPCC (2013) *Climate Change 2013: The Physical Science Basis. Contribution of Working Group I to the Fifth Assessment Report of the Intergovernmental Panel on Climate Change* [Stocker TF, Qin D, Plattner G-K, Tignor M, Allen SK, Boschung J, Nauels A, Xia Y, Bex V, Midgley PM (eds.)]. Cambridge University Press, Cambridge, United Kingdom and New York, NY, USA, 1535 pp.

28. IPCC (2021) Summary for Policymakers. In: Climate Change 2021: The Physical Science Basis. Contribution of Working Group I to the Sixth Assessment Report of the Intergovernmental Panel on Climate Change [Masson-Delmotte V, Zhai P, Pirani A, Connors SL, Péan C, Berger S, Caud N, Chen Y, Goldfarb L, Gomis MI, Huang M, Leitzell K, Lonnoy E, Matthews JBR, Maycock TK, Waterfield T, Yelekçi O, Yu R, Zhou B (eds.)]. Cambridge University Press. In Press.
29. James R, Washington R, Abiodun B, Kay G, Mutemi J, Pokam W, Hart N, Artan G Senior C (2018) Evaluating climate models with an African lens. Bull AmerMeteorolSoc 99: 313–336. https://doi.org/10.1175/BAMS-D-16-0090.1
30. Kendall MG (1975) Rank correlation methods, 4thEdn. Griffin, London, pp. 202
31. King JA, Washington R, Engelstaedter S (2021) Representation of the Indian Ocean Walker circulation in climate models and links to Kenyan rainfall. Int J Climatol 41: E616–E643. https://doi.org/10.1002/joc.6714
32. Knutti R, Furrer R, Tebaldi C, Cermak J, Meehl GA (2010) Challenges in combining projections from multiple climate models. J Climate 23: 2739–2758. https://doi.org/10.1175/2009JCLI3361.1
33. Knutti R, SedláčekJ, SandersonBM,et al (2017) A climatemodel projection weighting scheme accounting for performance and interdependence. Geophys. Res. Lett., 44, 19091918, doi: 10.1002/2016GL072012
34. Krasting JP, John JG, Blanton C, McHugh C, Nikonov S, Radhakrishnan A, Rand K, Zadeh NT, Balaji V, Durachta J, Dupuis C, Menzel R, Robinson T, Underwood S, Vahlenkamp H, Dunne KA, Gauthier PPG, Ginoux P, Griffies SM, Hallberg R, Harrison M, Hurlin W, Malyshev S, Naik V, Paulot F, Paynter DJ, Ploshay J, Reichl BG, Schwarzkopf DM, Seman CJ, Silvers L, Wyman B, Zeng Y, Adcroft A, Dunne JP, Dussin R, Guo H, He J, Held IM, Horowitz LW, Lin P, Milly PCD, Shevliakova E, Stock C, Winton M, Wittenberg AT, Xie Y, Zhao M (2018) NOAA-GFDL GFDL-ESM4 model output prepared for CMIP6 CMIP historical. Earth System Grid Federation, Version 20200306. https://doi.org/10.22033/ESGF/CMIP6.8597
35. Liebmann B, Hoerling MP, Funk C, Bladé I, Dole, RM, Allured D, Quan X, Pegion P, Eischeid, JK (2014) Understanding recent eastern Horn of Africa rainfall variability and change. J Climate 27: 8630–8645. https://doi.org/10.1175/JCLI-D-13-00714.1
36. Lim Kam Sian KTC, Wang J, Ayugi B, Nooni IK, Ongoma V (2021) Multi-decadal variability and future changes in precipitation over Southern Africa. Atmosphere 12: 742. https://doi.org/10.3390/atmos12060742
37. Limantol AM, Keith BE, Azabre BA, Lennartz B (2016) Farmers' perception and adaptation practice to climate variability and change: a case study of the Vea catchment in Ghana. SpringerPlus 5, 830.https://doi.org/10.1186/s40064-016-2433-9
38. Luo N, Guo Y, Gao Z, Chen K, Chou J (2020) Assessment of CMIP6 and CMIP5 model performance for extreme temperature in China. Atmos. Oceanic Sci Lett 13: 589–597. https://doi.org/10.1080/16742834.2020.1808430

39. Lyon B (2014) Seasonal drought in the Greater Horn of Africa and its recent increase during the March–May long rains. J Climate 27: 7953–7975. https://doi.org/10.1175/JCLI-D-13-00459.1
40. Mann HB (1945) Nonparametric tests against trend. Econometrica 13: 245–259.
41. Makula EK, Zhou B (2021) Coupled Model Intercomparison Project phase 6 evaluation and projection of East African precipitation. Int J Climatol. https://doi.org/10.1002/joc.7373
42. Mulinde C, Majaliwa JGM, Twesigomwe E, Egeru A (2016) Meteorological drought occurrence and severity in Uganda. In Nakileza BR, Bamutaze Y, Mukwaya P (Eds.), *Disasters and Climate Resilience in Uganda: Processes, Knowledge and Practices* (pp. 185–215). Kampala, Uganda: UNDP.
43. Mumo L, Yu J, Ayugi B (2019) Evaluation of spatiotemporal variability of rainfall over Kenya from 1979 to 2017. J Atmos Sol Terr Phys 105097. https://doi.org/10.1016/j.jastp.2019.105097
44. National Environment Management Authority (NEMA) 2008. State of Environment Report for Uganda, 2008, National Environment Management Authority, Kampala, pp. 282.
45. NBER (2010) *Agriculture, Roads, and Economic Development in Uganda.* Cambridge, MA: National Bureau of Economic Research. http://www.nber.org/papers/w15863 (Accessed 05 May 2021)
46. Ngarukiyimana JP, Fu Y, Yang Y, Ogwang BA, Ongoma V, Ntwali D (2017) Dominant atmospheric circulation patterns associated with abnormal rainfall events over Rwanda, East Africa. Int J Climatol 38: 187–202. https://doi.org/10.1002/joc.5169
47. Ngoma H, Wen W, Ayugi B, Babaousmail H, Karim R, Ongoma V (2021c) Evaluation of rainfall simulations in CMIP6 models over Uganda. Int J Climatol 41:4743–4768. https://doi.org/10.1002/joc.7098
48. Ngoma H, Wen W, Ayugi B, Karim R, Makula EK (2021b) Mechanisms associated with September to November (SON) rainfall over Uganda during the recent decades. GeographicaPannonica25: 10-23.https://doi.org/10.5937/gp25-29932
49. Ngoma H, Wen W, Ojara M, Ayugi B (2021a) Assessing current and future spatiotemporal rainfall variability and trends over Uganda, East Africa based on CHIRPS and Regional Climate Models Datasets. MeteorolAtmosPhys133: 823–843. https://doi.org/10.1007/s00703-021-00784-3
50. Nicholson SE (2015) Long-term variability of the East African “short rains” and its links to large-scale factors. Int J Climatol 35: 3979–3990. https://doi.org/10.1002/joc.4259
51. Nicholson SE (2018) The ITCZ and the Seasonal Cycle over Equatorial Africa. Bull Amer Meteor Soc 99: 337–348. https://doi.org/10.1175/BAMS-D-16-0287.1
52. Nicholson SE, Kim J (1997) The relationship of the El Niño–Southern Oscillation to African rainfall. Int J Climatol 17: 117–135. https://doi.org/10.1002/(SICI)1097-0088(199702)17:2<117::AID-JOC84>3.0.CO;2-O.
53. Nimusiima A, Basalirwa CPK, Majaliwa JGM, Mbogga SM, Mwavu EN, Namaalwa J, Okello-Onen J (2014) Analysis of future climate scenarios over central Uganda cattle corridor. J Earth SciClim Change 5, 10. https://doi.org/10.4172/2157-7617.1000237

54. Nimusiima A, Kisembe J, Nakyembe N (2019) Evaluation of past and future extreme rainfall characteristics over Eastern Uganda. J Environ Agric Sci 18: 38–49.
55. Nsubuga FNW, Olwoch JM, de Rautenbach CJW, Botai OJ (2014) Analysis of mid-twentieth century rainfall trends and variability over southwestern Uganda. TheorApplClimatol 115: 53–71. https://doi.org/10.1007/s00704-013-0864-6
56. Nsubuga FNW, Rautenbach H (2017) Climate change and variability: a review of what is known and ought to be known for Uganda. Int J Clim Chang Str 10: 752–771. https://doi.org/10.1108/IJCCSM-04-2017-0090
57. O'Neill BC, Kriegler E, Ebi KL, Kemp-Benedict E, Riahi K, Rothman DS, van Ruijven BJ, van Vuuren DP, Birkmann J, Kok K, Levy M, Solecki W (2017) The roads ahead: narratives for Shared Socioeconomic Pathwaysdescribing world futures in the 21st century. Global Environ. Change 42: 169–180.https://doi.org/10.1016/j.gloenvcha.2015.01.004
58. Ogwang BA, Ongoma V, Xing L, Ogou FK (2015) Influence of Mascarene high and Indian Ocean dipole on East African extreme weather events. GeographicaPannonica 19: 64–72. https://doi.org/10.5937/geopan1502064o
59. Ojara MA, Lou Y, Aribo L, Namumbya S, Uddin MJ (2020) Dry spells and probability of rainfall occurrence for Lake Kyoga Basin in Uganda, East Africa. Nat Hazards 100:493–514. https://doi.org/10.1007/s11069-019-03822-x
60. Ongoma V, Chen H (2017) Temporal and spatial variability of temperature and rainfall over East Africa from 1951 to 2010. MeteorolAtmosPhys129: 131–144. https://doi.org/10.1007/s00703-016-0462-0
61. Ongoma V, Chen H, Gao C (2018) Projected change in mean rainfall and temperature over East Africa based on CMIP5 Models. Int J Climatol 38: 1375–1392. http://doi.org/10.1002/joc.5252
62. Ongoma V, Rahman MA, Ayugi B, Nisha F, Galvin S, Shilenje ZW, Ogwang BA (2021) Variability of diurnal temperature range over Pacific Island countries, a case of Fiji. MeteorolAtmosPhys 133: 85–95. https://doi.org/10.1007/s00703-020-00743-4
63. Onyutha C (2016) Geospatial Trends and Decadal Anomalies in Extreme Rainfall over Uganda, East Africa. AdvMeteorol 2016, 6935912. https://doi.org/10.1155/2016/6935912
64. Onyutha C (2018) African crop production trends are insufficient to guarantee food security in the sub-Saharan region by 2050 owing to persistent poverty. Food Sec 10: 1203–1219. https://doi.org/10.1007/s12571-018-0839-7
65. Onyutha C (2019) African food insecurity in a changing climate: The roles of science and policy. Food Energy Sec 8, e00160.https://doi.org/10.1002/fes3.160
66. Onyutha C, Asiimwe A, Ayugi B, Ngoma H, Ongoma V, Tabari H (2021) Observed and Future Precipitation and Evapotranspiration in Water Management Zones of Uganda. CMIP6 Projections. Atmosphere 12, 887. https://doi.org/10.3390/atmos12070887
67. Onyutha C, Tabari H, Rutkowska A, Nyeko-Ogiramoi P, Willems P (2016) Comparison of different statistical downscaling methods for climate change rainfall projections over the Lake Victoria basin

considering CMIP3 and CMIP5. J Hydro-environ Res 12: 31–45. https://doi.org/10.1016/j.jher.2016.03.001

68. Patricola CM, Cook KH (2011) Sub-Saharan northern African climate at the end of the twenty-first century: forcing factors and climate change processes. ClimDyn37: 1165–1188. https://doi.org/10.1007/s00382-010-0907-y
69. Reliefweb (2021) Uganda: Floods and Landslides - Sep 2021. FL-2021-000153-UGA. https://reliefweb.int/disaster/fl-2021-000153-uga(Accessed 22nd March 2022)
70. Riahi K, Vuuren DP, Kriegler E, Edmonds J, O'Neill BC, Fujimori S, Bauer N, Calvin K, Dellink R, Fricko O, Lutz W (2017) The shared socioeconomic pathways and their energy, land use, and greenhouse gas emissions implications: an overview. Global Environ. Change 42: 153–168. https://doi.org/10.1016/j.gloenvcha.2016.05.009
71. Rowell DP, Booth BBB, Nicholson SE, Good P (2015) Reconciling past and future rainfall trends over East Africa. J Climate 28: 9768–9788. https://doi.org/10.1175/JCLI-D-15-0140.1
72. Sanderson BM, Knutti R, Caldwell P (2015) A representative democracy to reduce interdependency in a multimodel ensemble. J Climate 28: 5171–5194. https://doi.org/10.1175/JCLI-D-14-00362.1
73. Saji NH, Goswami BN, Vinayachandran PN, Yamagata T (1999) A dipole mode in the tropical Indian ocean. Nature 401: 360–363. https://doi.org/10.1038/43854
74. Seland Ø, Bentsen M, Olivié D, Toniazzo T, Gjermundsen A, Graff LS, Debernard JB, Gupta AK, He Y, Kirkevåg A, Schwinger J, Tjiputra J, Aas KS, Bethke I, Fan Y, Griesfeller J, Grini A, Guo C, Ilicak M, Karset IHH, Landgren O, Liakka J, Moseid KO, Nummelin A, Spensberger C, Tang H, Zhang Z, Heinze C, Iversen T, Schul M (2020) The Norwegian Earth System Model, NorESM2—Evaluation of the CMIP6 DECK and his- torical simulations. Geosci Model Dev, Discussion. https://doi.org/10.5194/gmd-2019-378.
75. Sen PK (1968) Estimates of the regression coefficient based on Kendall's tau. J Am Stat Assoc 63: 1379–1389. https://doi.org/10.2307/2285891.
76. Sillmann J, Kharin VV, Zhang X, Zwiers FW, Bronaugh D (2013) Climate extremes indices in the CMIP5 multimodel ensemble: Part 1. Model evaluation in the present climate. J Geophys Res Atmos 118: 1716–1733. https://doi.org/10.1002/jgrd.50203
77. Sneyers R (1990) On the Statistical Analysis of a Series of Observations. Tech Note 143: WMO-No. 415, 192
78. Stott PA, Christidis N, Otto FEL, Sun Y, Vanderlinden J, Oldenborgh GJ, Vautard R, Storch H, Walton P, Yiou P, W Zwiers FW (2013) Attribution of extreme weather and climate-related events. Wiley Interdiscip Rev Clim Chang 7:23–41. https://doi.org/10.1002/wcc.380
79. Stouffer R, Eyring V, Meehl G, Bony S, Senior C, Stevens B, Taylor K (2016) CMIP5 scientific gaps and recommendations for CMIP6. Bull Amer Meteor Soc 98: 95–105. https://doi.org/10.1175/BAMS-D-15-00013.1
80. Swart NC, Cole JNS, Kharin VV, Lazare M, Scinocca JF, Gillett NP, Anstey J, Arora V, Christian JR, Hanna S, Jiao Y, Lee WG, Majaess F, Saenko OA, Seiler C, Seinen C, Shao A, Sigmond M, Solheim L,

von Salzen K, Yang D, Winter B (2019) The Canadian Earth System Model version 5 (CanESM5.0.3). Geosci Model Dev 12: 4823–4873. https://doi.org/10.5194/gmd-12-4823-2019.

81. Sylla MB, Giorgi F, Coppola E, Mariotti L (2012) Uncertainties in daily rainfall over Africa: assessment of gridded observation products and evaluation of a regional climate model simulation. Int J Climatol 33: 1805–1817. https://doi.org/10.1002/joc.3551
82. Tadeyo E, Chen D, Ayugi B, Yao C (2020) Characterization of Spatio-Temporal Trends and Periodicity of Rainfall over Malawi during 1979 - 2015. Atmosphere 11, 891 https://doi.org/10.3390/atmos11090891
83. Tan, G, Ayugi B, Ngoma H, Ongoma V (2020) Projections of future meteorological drought events under representative concentration pathways (RCPs) of CMIP5 over Kenya, East Africa. Atmos Res 246, 105112. http://dx.doi.org/10.1016/j.atmosres.2020.105112
84. Tebaldi C, Knutti R (2007) The use of the multi-model ensemble in probabilistic climate projections. Phil Trans Royal Soc A 365: 2053–2075. https://doi.org/10.1098/rsta.2007.2076.
85. Theil H (1950) A rank-invariant method of linear and polynomial regression analysis. I, II, III. Proc R Netherlands AcadSci53:Part I: 386-392, Part II: 521-525, Part III: 1397-1412
86. Tierney JE, Ummenhofer CC, DeMenocal PB (2015) Past and future rainfall in the Horn of Africa. Sci Adv 1: 1–9. https://doi.org/10.1126/sciadv.1500682
87. van Vuuren DP, Edmonds J, Thomson A, Kainuma M, Riahi K, Thomson A, Hibbard K, Hurtt, GC, Kram T, Krey V, Lamarque JF, Masui, T, Meinshausen M, Nakicenovic N, Smith S, Rose SK (2011) The Representative Concentration Pathways: an overview. Climatic Change 109: 5–31. https://doi.org/10.1007/s10584-011-0148-z
88. Vermeulen JL, Hillebrand A, Geraerts R (2017) A comparative study of k-nearest neighbour techniques in crowd simulation. ComputAnimat Virtual Worlds 28:e1775 .https://doi.org/10.1002/cav.1775
89. Voldoire A, Saint-Martin D, Sénési S, Decharme B, Alias A, Chevallier M, et al. (2019) Evaluation of CMIP6 DECK experiment with CNRM-CM6-1. J Adv Model Earth Syst 11: 2177–2213. https://doi.org/10.1029/2019MS001683.
90. WFP (2016) *Uganda: Current issues and what the World Food Programme is doing.* Rome, Italy: The World Food Programme. http://www.wfp.org/countries/uganda (Accessed 05 May 2021)
91. Williams AP, Funk C (2011) A westward extension of the warm pool leads to a westward extension of the Walker circulation, drying eastern Africa. ClimDyn 37: 2417–2435. https://doi.org/10.1007/s00382-010-0984-y
92. Yang W, Seager R, Cane MA, Lyon B (2015) The rainfall annual cycle bias over East Africa in CMIP5 coupled climate models. J Climate 28: 9789–9802. https://doi.org/10.1175/JCLI-D-15-0323.1.
93. Yukimoto S, Koshiro T, Kawai H, Oshima N, Yoshida K, Urakawa S, Tsujino H, Deushi M, Tanaka T, Hosaka M, Yoshimura H, Shindo E, Mizuta R, Ishii M, Obata A, Adachi Y (2019) MRI MRI-ESM2.0 model output prepared for CMIP6 CMIP historical. Earth System Grid Federation. Version 20200430. https://doi.org/10.22033/ESGF/CMIP6.6842.

94. Zhang L, Wu P, Zhou T, Roberts MJ, Schiemann R (2016) Added value of high resolution models in simulating global precipitation characteristics. Atmos Sci Lett 17: 646–657. https://doi.org/10.1002/asl.715

95. Zhu HH, Jiang ZH, LI J, Li W, Sun CX, Li L (2020) Does CMIP6 inspire more confidence in simulating climate extremes over China? Adv Atmos Sci 37: 1119–1132. https://doi.org/10.1007/s00376-020-9289-1

Figures

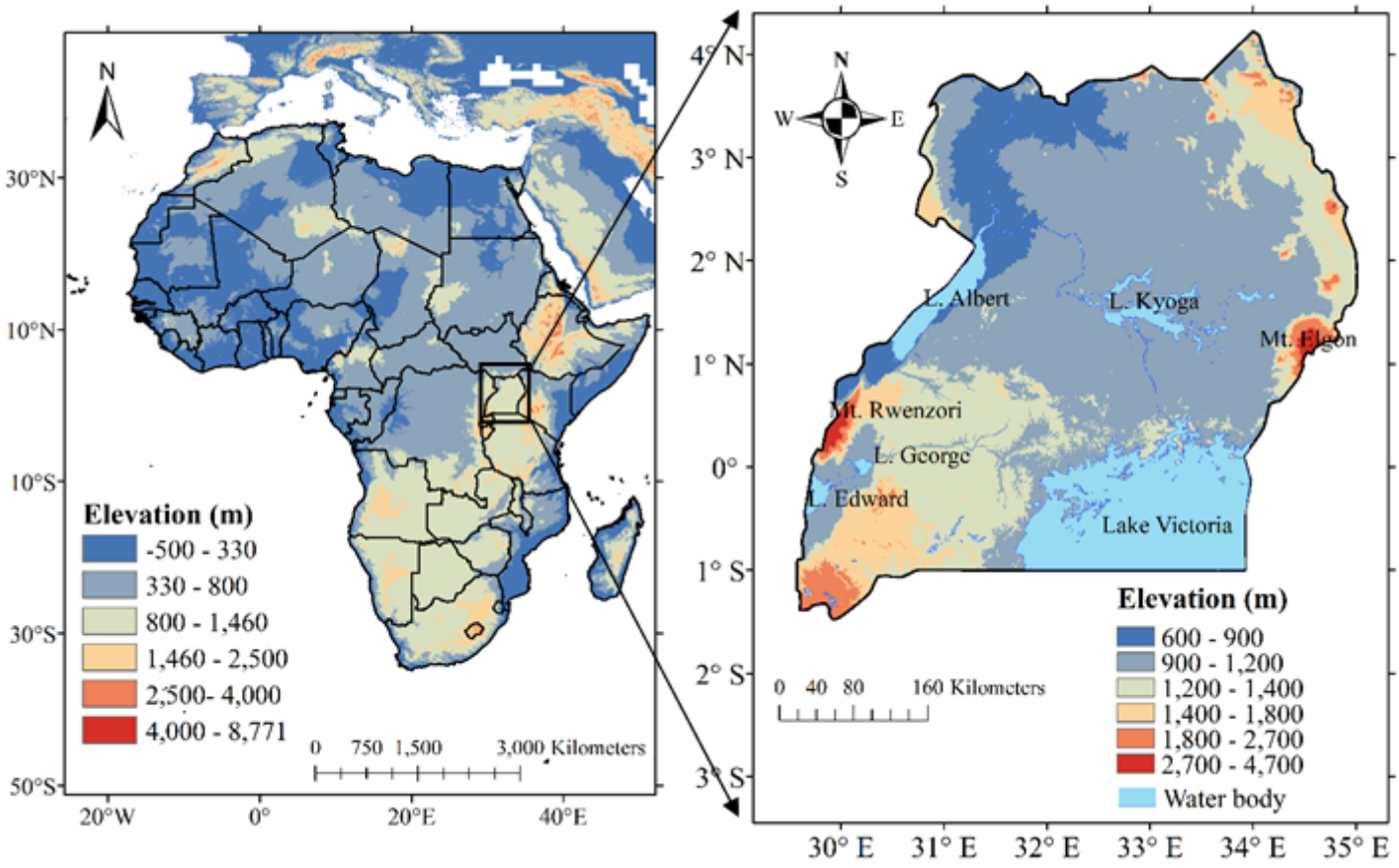

Figure 1

Uganda's elevation (m), geophysical features andthe country's location in the African continent.

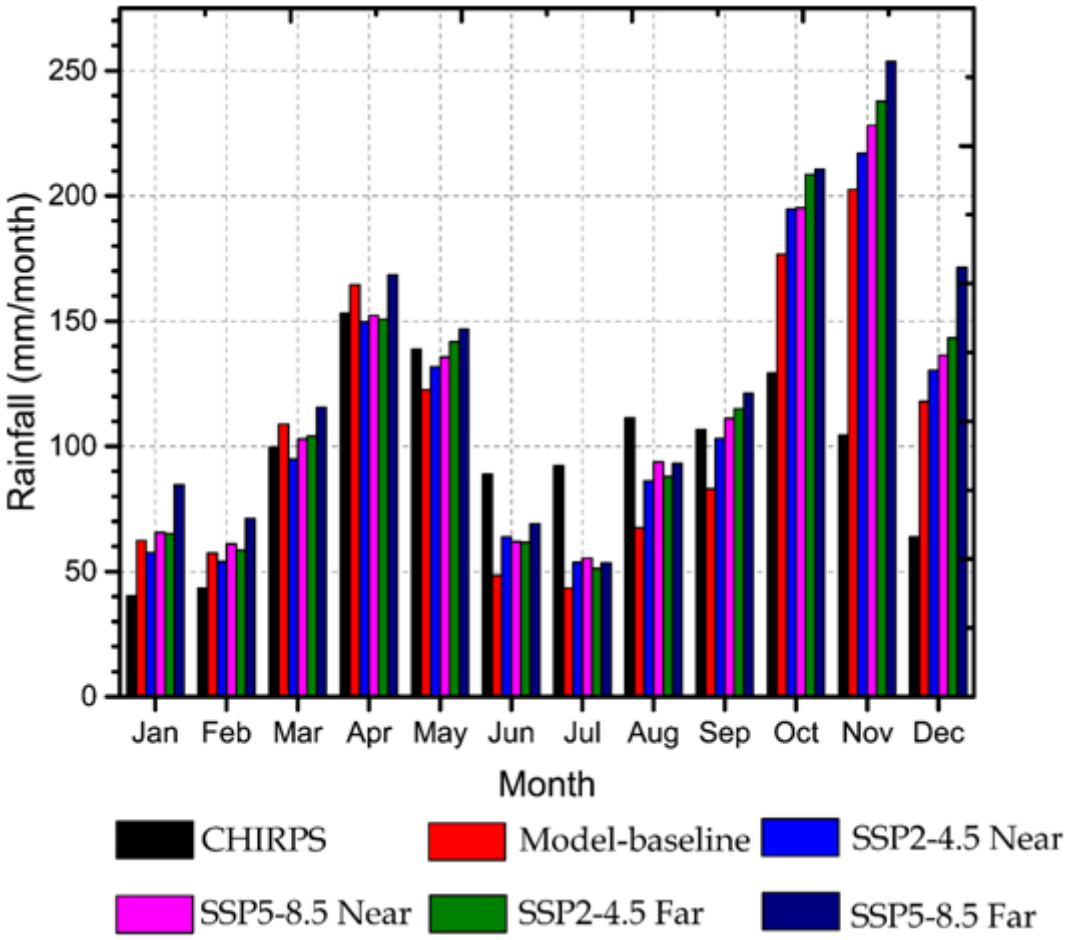

Figure 2

Monthly rainfall climatology for 1985–2014 over Uganda based on observed (CHIRPS in black) and model ensemble (red), and for the projected period of 2021 – 2060, 2061 – 2100 under the SSP 2-4.5(blue and green) and 5-8.5 (magenta and dark blue) emission scenarios.

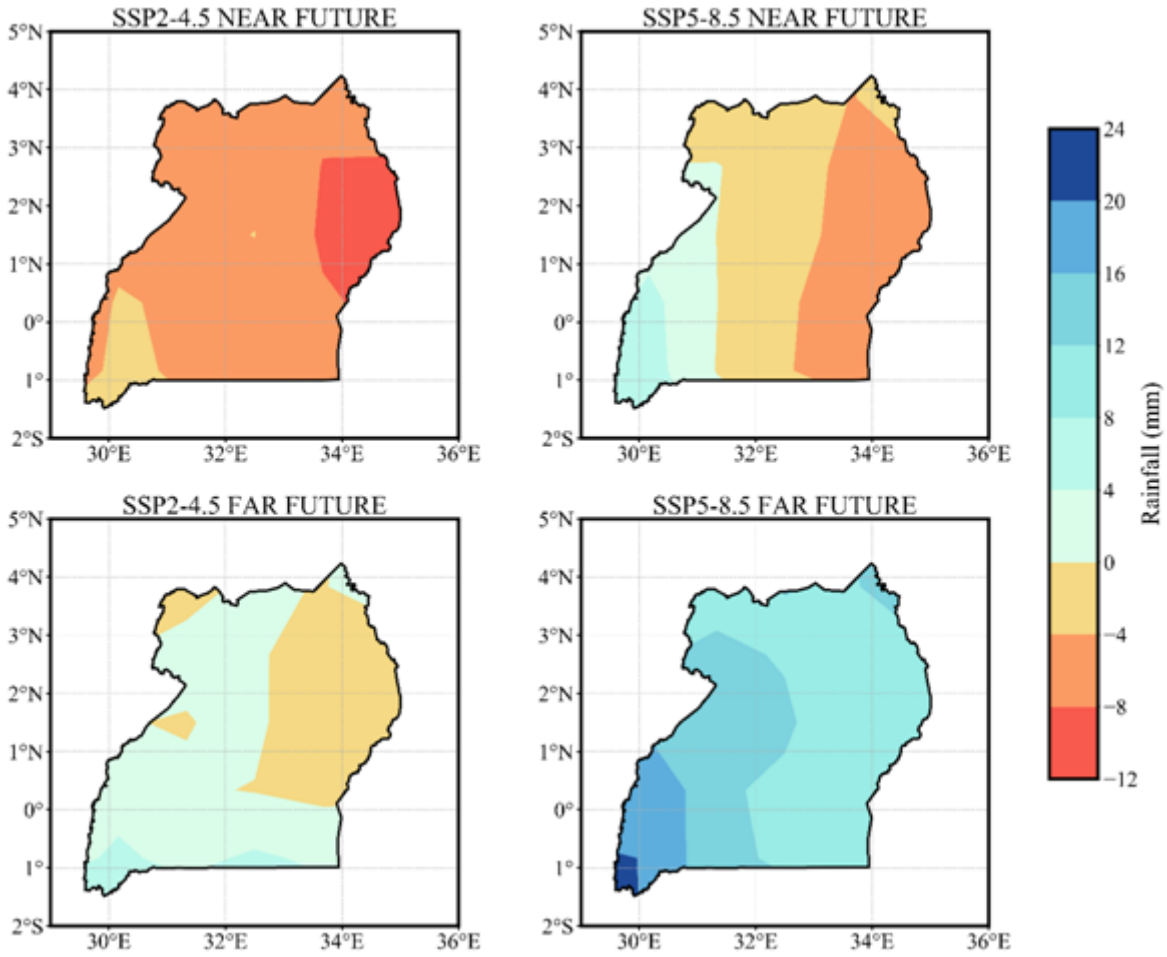

Figure 3

Projected percentage changes in MAM rainfall (mm) over Uganda relative to the baseline period (1985 – 2014) for the near and far future under the SSP2-4.5 and SSP5-8.5emission scenarios.

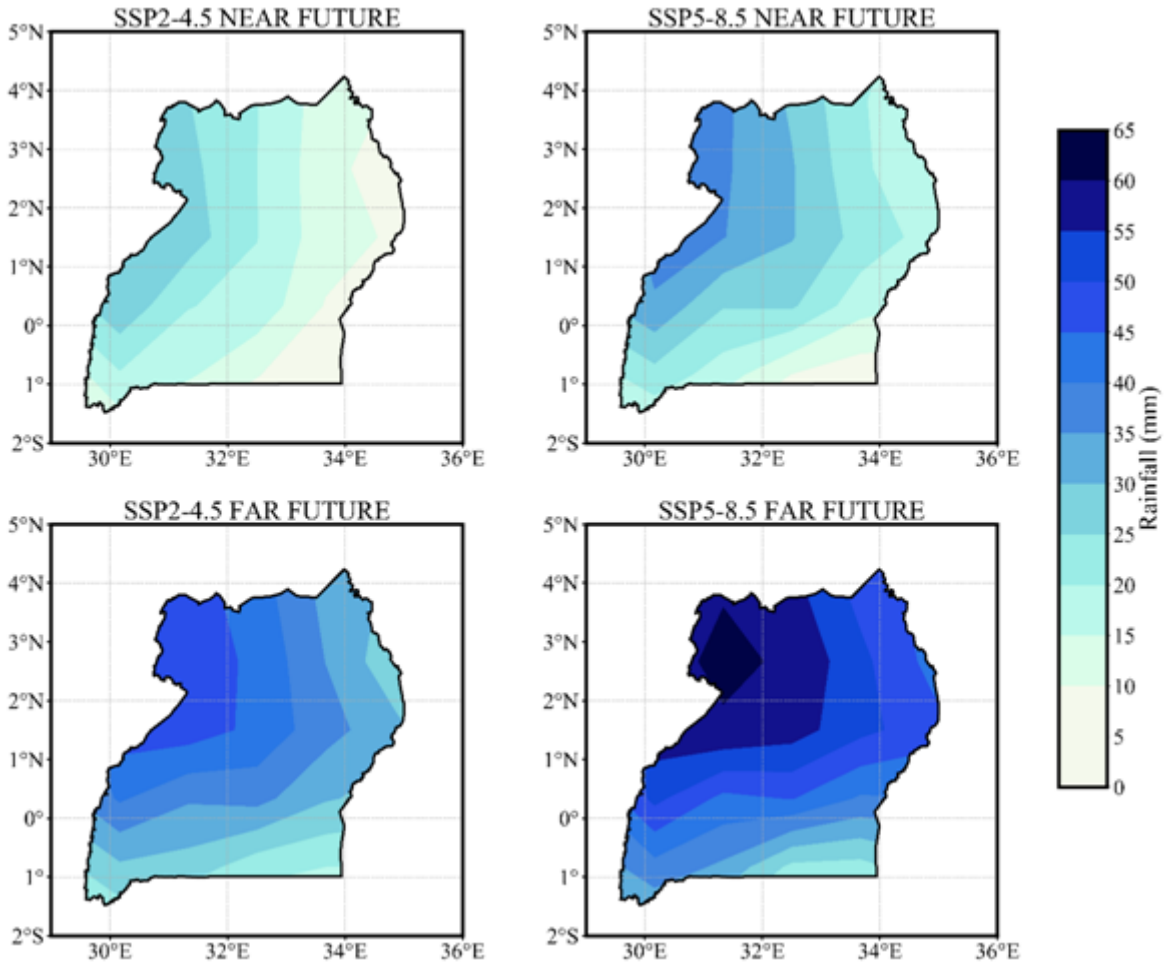

Figure 4

Same as Figure 3, but for SON.

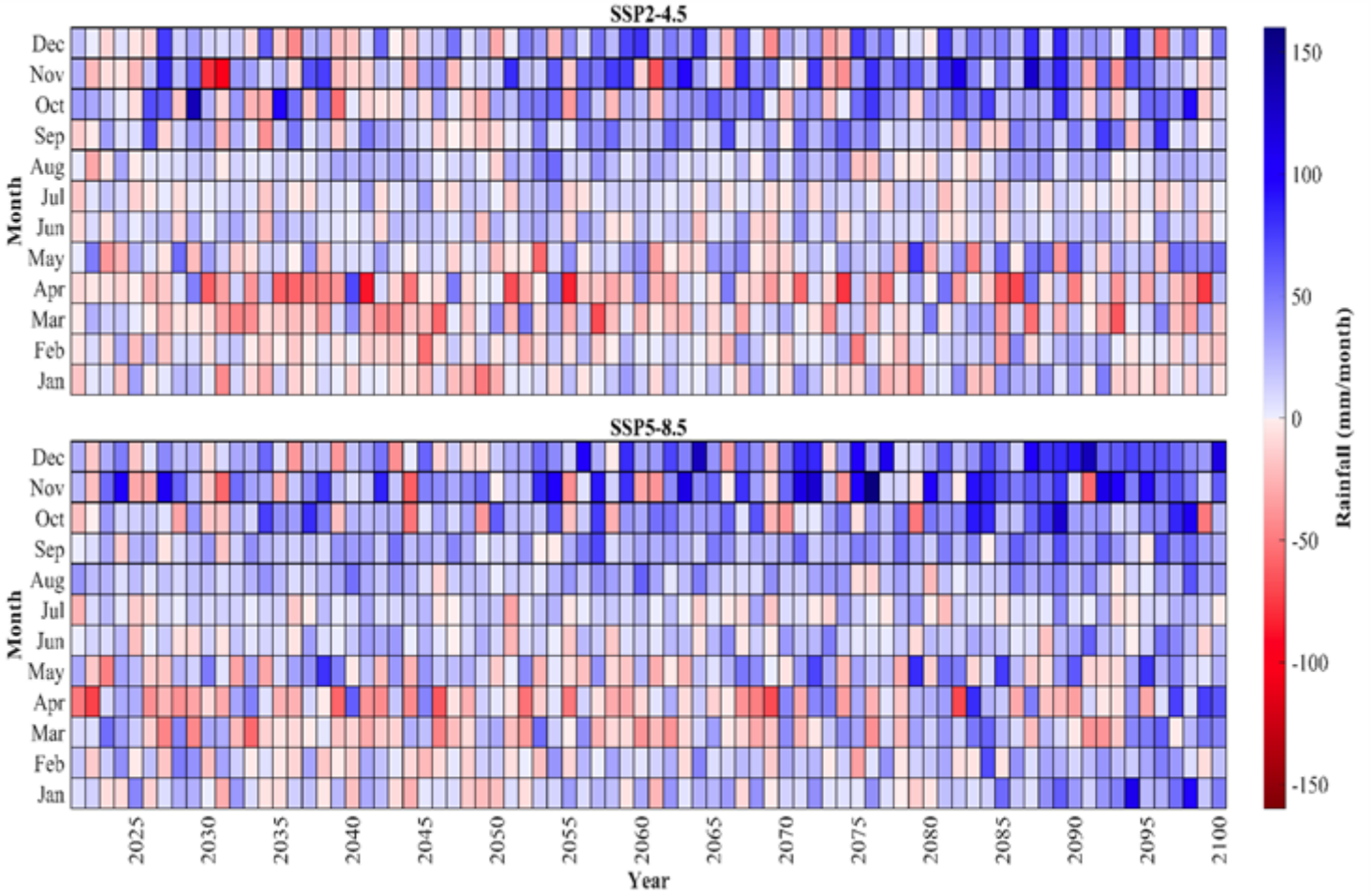

Figure 5

Portrait diagram for projected change in rainfall over Uganda for 2021 – 2100 under SSP2-4.5 andSSP5-8.5 relative to thebaseline period (1985 – 2014).

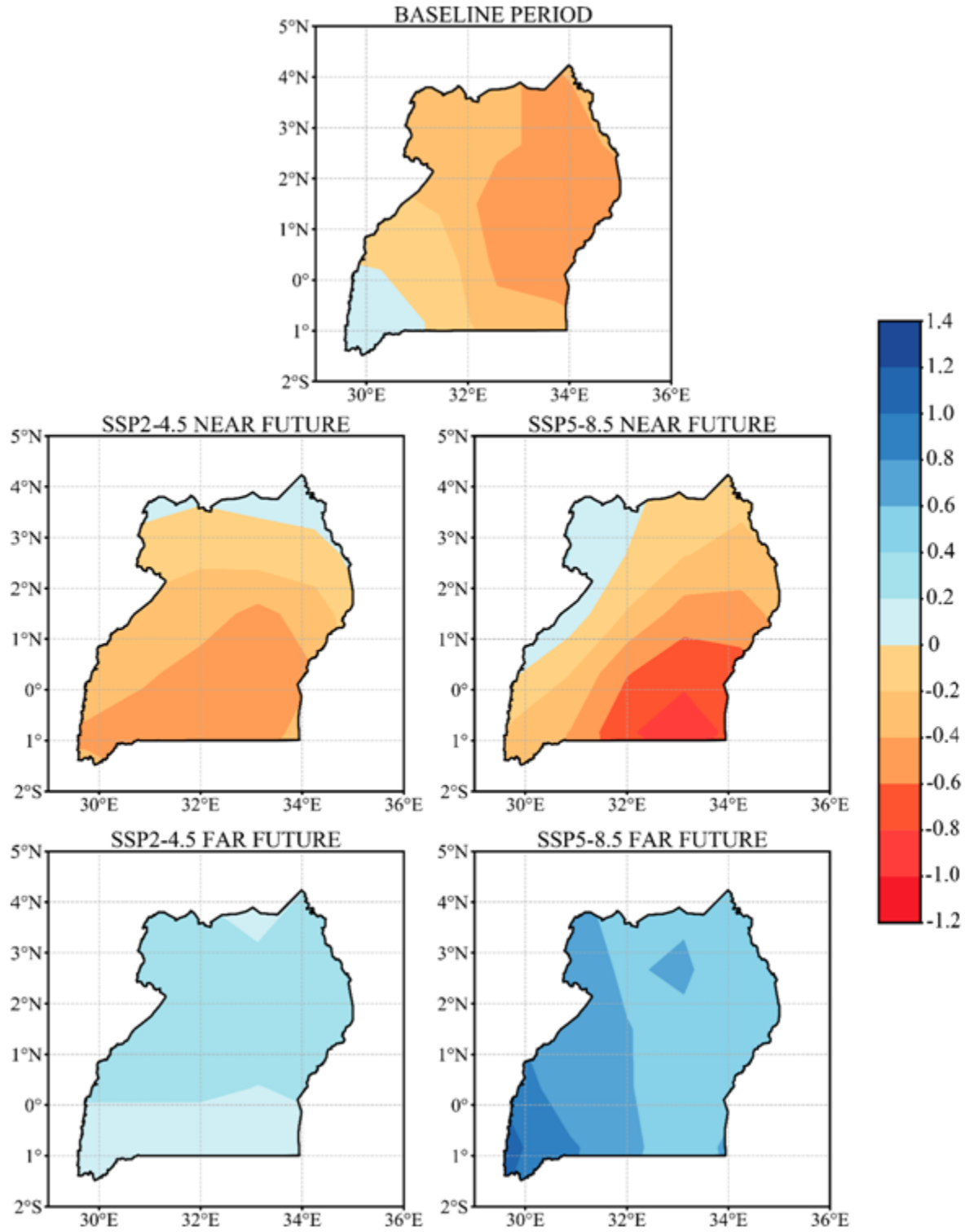

Figure 6

Spatial pattern ofprojected linear trend forMAM rainfall over Uganda based on CMIP6 ensemble mean during 2021 – 2060 and 2061 – 2100 relative to the baselineperiod (1985–2014).

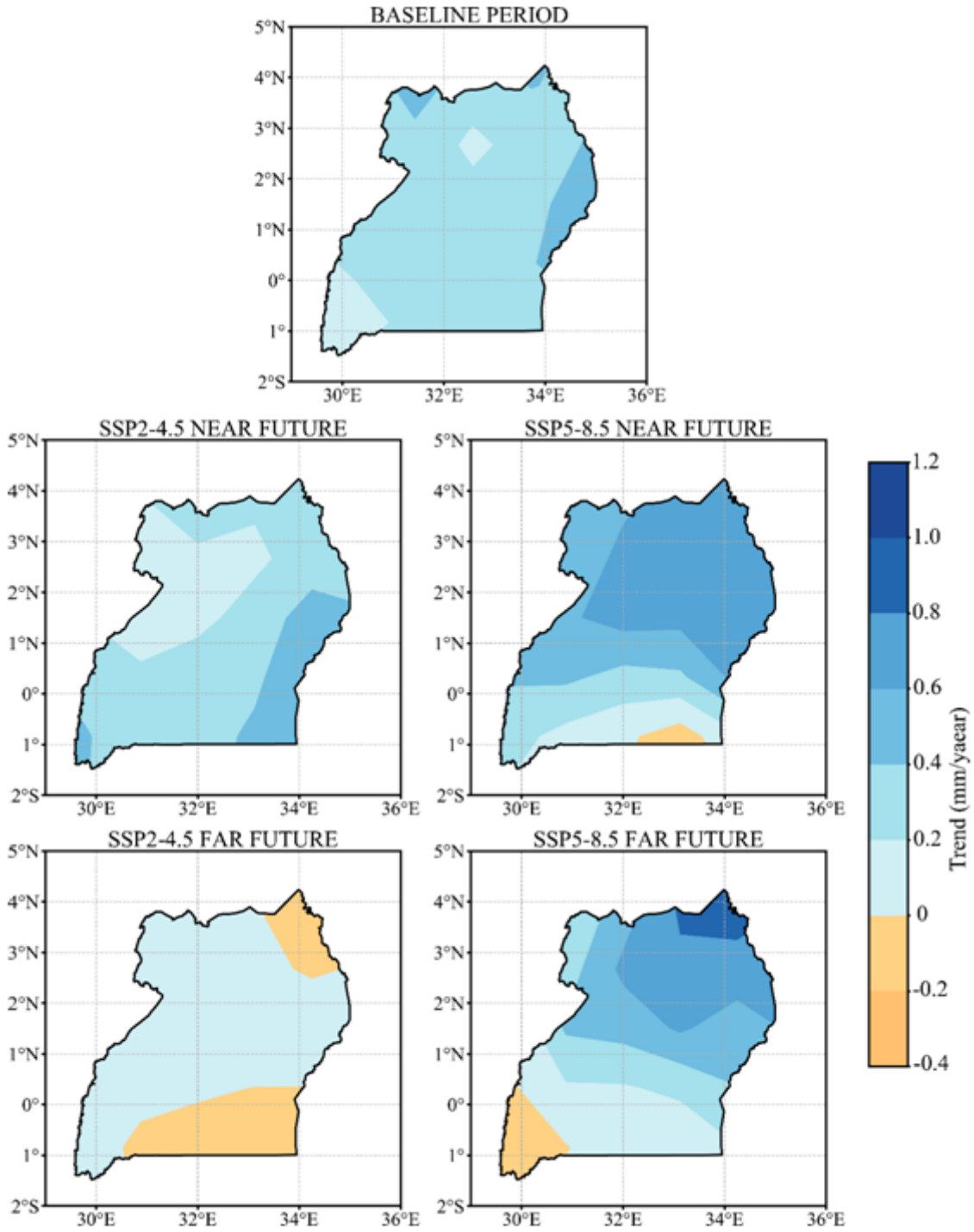

Figure 7

Same as Figure 6, but for SON.

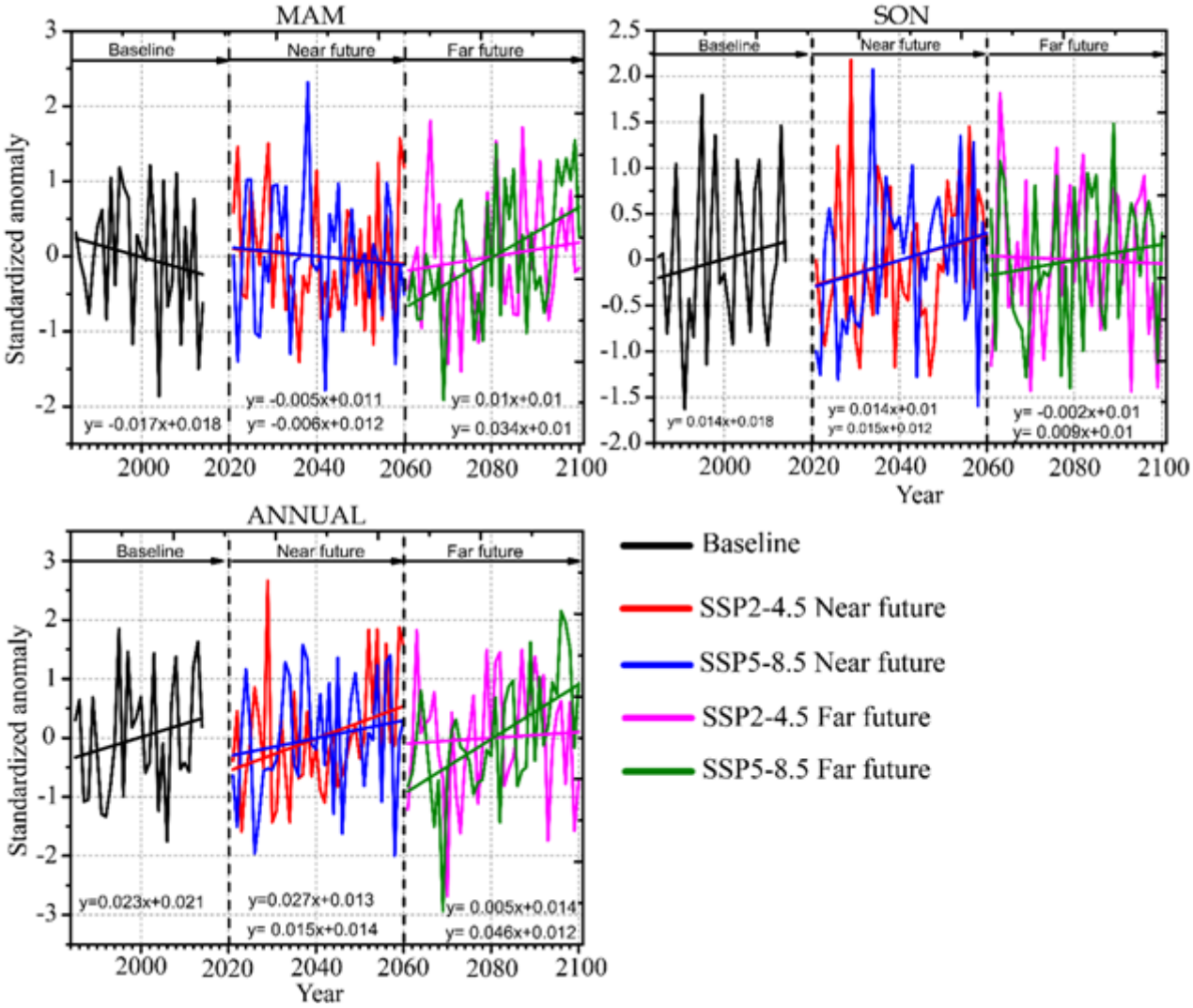

Figure 8

Projected rainfall anomalies over Uganda under SSPs 2-4.5 and 5-8.5 for 2021 – 2100 relative to the baseline period (1985-2014).

Figure 9

Sequential Mann-Kendall ofprojected rainfall for MAM (a,b), SON (c,d) and annual (e,f) rainfall over Uganda under SSPs 2-4.5 and 5-8.5 for the period 2021 – 2100.

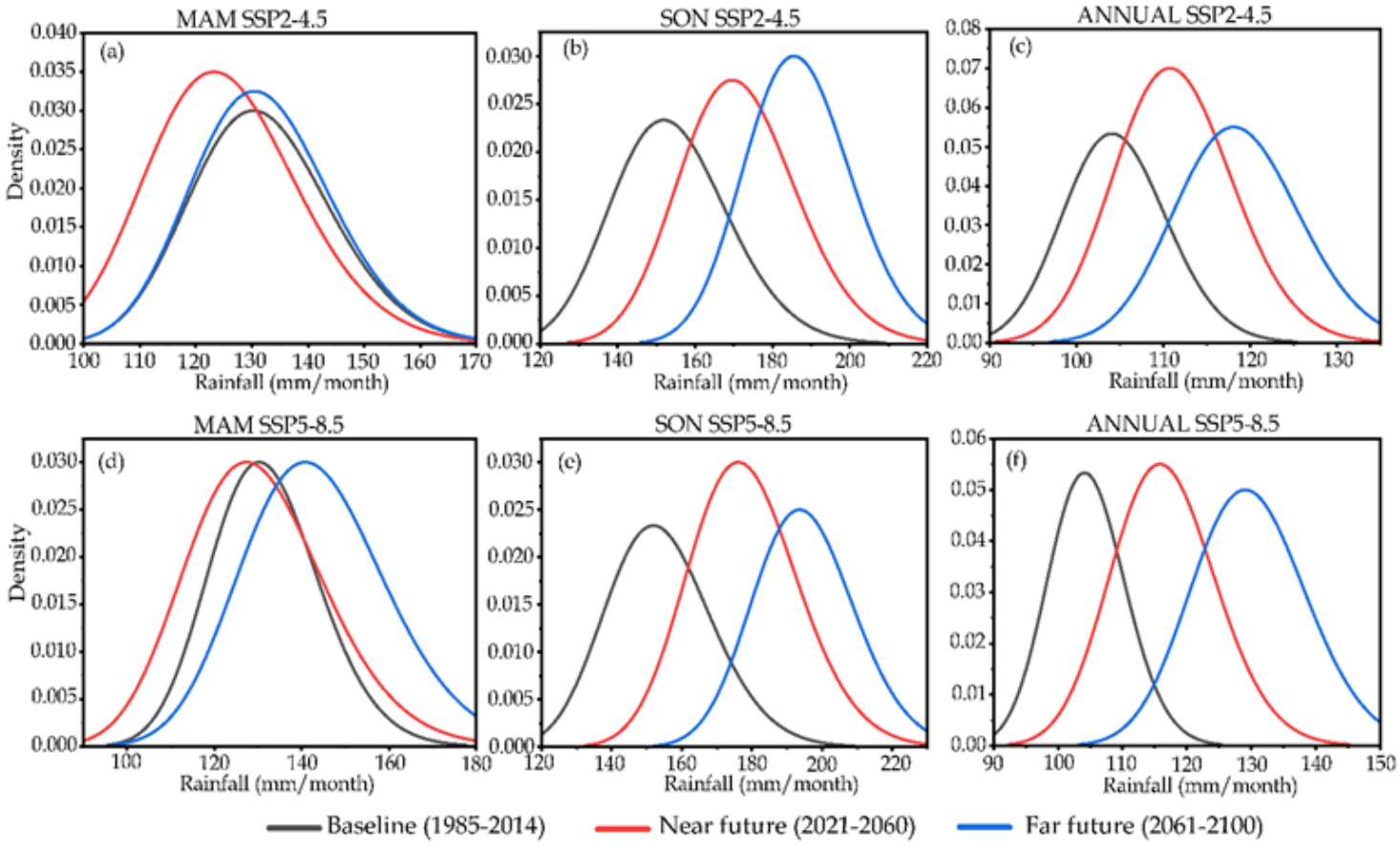

Figure 10

Probability density functions (PDFs) for seasonal (MAM and SON) and annual rainfall for the baseline period (black line), and2021-2060 (red line) and 2061-2100 (blue line) under SSPs 2-4.5 (a-c) and 5-8.5 (d-f) over Uganda.